ACS OMEGA

Open Access

http://pubs.acs.org/journal/acsodf

Article

Synergistic Inhibition of Colon Cancer Cell Proliferation via p53, Bax, and Bcl-2 Modulation by Curcumin and Plumbagin Combination

Iftikhar Ahmad, Sameer Ahmad, Md Abdus Samad, Ahmed Mohammed Adam, Torki A. Zughaibi, Mahmoud Alhosin, Shazi Shakil, Mohd Shahnawaz Khan, Ahdab A. Alsaieedi, Ajoy Kumer,* and Shams Tabrez*

Cite This: *ACS Omega* 2025, 10, 19045−19060

Read Online

ACCESS | Metrics & More | Article Recommendations

ABSTRACT: Cancer is a major contributor to global morbidity and mortality. Among the different forms of cancer, colorectal cancer (CRC) is the third most frequently diagnosed cancer in men and the second most common cancer type in women globally. We aimed to explore the possible synergistic anticancer potential of curcumin (Cur) and plumbagin (PL) in the human colon cancer cell line (HCT-116). The 3-(4,5-dimethylthiazol-2-yl)-2,5-diphenyltetrazolium bromide (MTT)/cytotoxicity assay revealed IC_{50} values of 7.7 and 7.5 μM for Cur and PL, respectively, as a separate entity. However, the combined treatment of Cur + PL significantly enhanced the cancer cell growth inhibitory potential compared with solitary treatments with an IC_{50} value of 6.8 μM. The combined treatment also led to the induction of apoptosis by 41%, cell cycle arrest at the G2/M phase, while Bax and p53 genes were found to be upregulated and the Bcl-2 gene was downregulated compared to the untreated/solvent control. Furthermore, combined treatment elevated reactive oxygen species (ROS) production by 59% and resulted a decline in the mitochondrial membrane potential (MMP) compared to the control. Catalase and superoxide dismutase (SOD) activities were significantly reduced, leading to enhanced lipid peroxidation (LPO) and compromised membrane integrity, which were also confirmed by 4′,6-diamidino-2-phenylindole (DAPI) + propoidium iodide (PI) staining were also noted. Our *in vitro* data were further supported by molecular docking, which showed a higher binding energy of the proteins (Bax, Bcl-2, and p53) with Cur + PL. Overall, our findings highlight the potent synergistic effects of the Cur and PL combination, which can be exploited as a combination therapy for CRC.

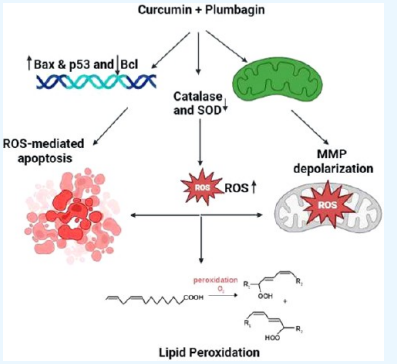

1. INTRODUCTION

Cancer is a profoundly challenging disease that affects millions of people globally and requires advancements in prevention, diagnosis, and treatment. Among the different forms of cancer, colorectal cancer (CRC) is the third most prevalent malignancy and the fourth leading cause of cancer-related mortality worldwide.[1] Despite significant advancements in diagnosis and treatment, CRC incidence and mortality rates remain unacceptably high.[2] The development of CRC is linked to several factors such as age, chronic health conditions, lifestyle, and reduced physical activity.[3,4] Current treatment approaches for CRC are tailored to the cancer stage and severity of complications, often relying on the success of chemotherapy, either as a standalone treatment or in combination with surgical resection or radiation therapy. While early-stage CRC responds well to treatments, such as radiotherapy and radical surgery, the prognosis for advanced cases is mainly chemotherapy-based and remains poor due to limited chemosensitivity.[5] Overall, CRC is challenging to treat and is associated with a high likelihood of recurrence.

Lately, there has been a growing focus on identifying natural compounds that are safe, affordable, and can be used alongside standard cancer drugs.[6,7] These plant-derived compounds can enhance the efficacy of current therapies and provide better acceptance among patients. Curcumin (Cur), or diferuloyl methane, is a hydrophobic polyphenol obtained from *Curcuma longa*, and is known for its antioxidant, anti-inflammatory, and chemotherapeutic properties.[8] Although several preclinical and clinical studies have reported its anticancer potential, there are concerns regarding its selectivity and bioavailability following oral administration. Curcumin's low bioavailability is mainly attributed to its chemical instability, limited absorption, rapid metabolism, and swift systemic clearance.[9,10] Similarly, plumbagin (PL) is a key bioactive compound (5-hydroxy-2-methyl-1,4-naphthoquinone) obtained from the roots of *Plumbago indica* and possesses several biological activities, such as anti-inflammatory, antioxidant, antifungal, antiproto-

Received: February 12, 2025
Revised: April 15, 2025
Accepted: April 24, 2025
Published: April 29, 2025

zoal, and antibacterial activities. Numerous studies have also reported its anticancer activity against different cancer models, which is largely linked to its ability to inhibit cell proliferation and induce apoptosis.[11,12] Its efficacy against a wide range of cancers, such as cervical cancer, lymphocytic leukemia, colon cancer, and hepatoma, has been well documented.[13−15] Although curcumin and plumbagin have been extensively studied for their individual anticancer properties in different cancer models, their possible utilization as a combination has yet to be explored. In continuation of earlier computational study, where we have reported the synergistic potential of plumbagin and curcumin combination, effectively targeting the PI3/Akt/mTOR pathway.[16] This study aims to explore the combined effects of curcumin and plumbagin against human colon cancer cell line (HCT-116) and understand the underlying mechanisms of their action.

2. MATERIALS AND METHODOLOGY

2.1. Reagents. For experimental purposes, a range of chemicals and kits was acquired from different suppliers.

Table 1. List of the Forward and Reverse Primer Sequences Used for RT-PCR

name of the gene	Primer sequence
Bax	Bax_(F): CATATAACCCCGTCAACGCAG
	Bax_(R): GCAGCCGCCACAAACATAC
Bcl-2	Bcl2_(F): ACAGGAGCTATACTCCAGGACA
	Bcl2_(R): GATCATACCCGTCATGGGGATA
p53	p53_(F): ACTTGTCGCTCTTGAAGCTAC
	p53_(R): GATGCGGAGAATCTTTGGAACA
GAPDH	GAPDH_(F): GGAGCGAGATCCCTCCAAAAT
	GAPDH_(R): GGCTGTTGTCATACTTCTCATGG

Paraformaldehyde, phosphate buffered saline (PBS), Dulbecco's modified Eagle medium (DMEM), dimethyl sulfoxide (DMSO), propidium iodide (PI), JC-1 dye, 4′,6-diamidino-2-phenylindole (DAPI), 3-(4,5-dimethylthiazol-2-yl)-2,5-diphenyltetrazolium bromide (MTT), trypsin, and CellRox were procured from Sigma-Aldrich (St. Louis, MO). RNA extraction, cDNA, SOD, catalase, lipid peroxidation (LPO), and Annexin V-FITC apoptosis kits were obtained from Thermo Fisher, USA and Abcam, China. All other reagents used in the experiments met analytical grade standards.

2.2. Cell Culture Maintenance. The American Type Culture Collection (ATCC, Manassas, VA) provided HCT-116 cells and PCS-201-013 cells (human lung fibroblast normal cells) for this study. These cellular components were cultivated under ideal conditions to promote robust growth and maintain experimental consistency. The aforementioned cell lines were cultured in high-glucose DMEM media enriched with 10% fetal bovine serum (FBS) and 1% antibiotic solution to prevent contamination. To mimic the physiological conditions necessary for optimal cell proliferation, the cells were maintained at 37 °C in a humidified incubator with controlled CO_2 levels. Before any experiments were conducted, cell viability was evaluated using a 0.4% trypan blue solution in PBS.

2.3. MTT Cytotoxicity Assay. The MTT colorimetric assay was used to evaluate cell viability by measuring the metabolic activity of living cells. In 96-well plates, HCT-116 and PCS-201-013 cells were plated at a concentration of 1×10^5 cells per well and allowed to adhere and proliferate for 24 h. After this initial incubation, the cells were exposed to varying concentrations of Cur (1−15 μM) and PL (1−15 μM), both separately and in combination, for 48 h. Subsequently, 5 μL of MTT reagent (5 mg/mL PBS) was added to each well, followed by a 2−2.5 h incubation period in a darkened environment. The resulting purple formazan crystals were solubilized by adding 50 μL of DMSO to each well. To ensure complete dissolution, the plate was kept in the dark for 15 min before measuring the absorbance at 490 nm using a microplate reader. The proportion of viable cells was determined by using the following equation:

$$\%\ \text{cell viability} = (\text{OD}_{490}\text{of the treatment} / \text{OD}_{490}\ \text{of the control}) \times 100$$

$$\%\ \text{growth inhibition} = 100 - \%\ \text{cell viability}$$

In addition, the therapeutic index of Cur and PL was calculated for PCS-201-013, as mentioned below

$$\text{therapeutic index} = \text{ED}_{50}/\text{TD}_{50}$$

ED_{50} = IC_{50} (50% Inhibitory concentration) = This is the concentration that reduces cell viability by 50%, representing the effective dose (ED_{50}).

TD_{50} = TC_{50} (50% Toxic concentration) = This is the concentration that reduces viability of normal cells by 50%, representing the toxic dose (TD_{50}).

2.4. Morphology Assay. A density of 1×10^3 cells per well was used to seed cells in 6-well plates. The cells were allowed to attach for 24 h at 37 °C in an environment containing 5% CO_2. Following this attachment phase, the cells were treated with IC_{50} concentrations of plumbagin, curcumin, or a combination of both and then incubated for an additional 24 h. After incubation, the culture medium was removed, and the cells were rinsed twice with 1× PBS to eliminate any remaining compounds. The cells were then fixed using 4% paraformaldehyde at 37 °C for 10 min. After fixation, a crystal violet solution was applied to cover the entire well surface and left for 20 min. The cells were subsequently washed again with 1× PBS to remove excess stain and inverted to completely dry. Finally, a compound microscope was used to observe morphological alterations in the cells, providing insights into how the compounds affected the cellular structure and integrity.

2.5. Wound Healing Assay. In 6-well plates, cells were plated at a density of 1×10^5 cells per well and left to adhere for 24 h in an incubator at 37 °C with 5% CO_2. Following this period, a scratch was created in the middle of each well using a sterile 10 μL pipette tip. The wells were washed twice with 1 × PBS to eliminate any loose cells, and the scratched area was observed under a compound microscope. New media containing IC_{50} concentrations of plumbagin, curcumin, or a combination of both was introduced into the wells, which were then incubated for an additional 24 h. Images of the scratch were captured at the beginning ($t = 0$) and end ($t = 24$) using a Zeiss microscope (Germany) at 10× magnification.

2.6. Mitochondrial Membrane Potential (MMP). Cells were plated in a 6-well plate at a density of 3×10^5 cells per well and allowed to adhere for 24 h. After this attachment period, the cells were exposed to IC_{50} concentrations of plumbagin, curcumin, or a combination of both. After treatment, the culture medium was removed by aspiration, and the cells were rinsed twice with 1× PBS to eliminate any

https://doi.org/10.1021/acsomega.5c01258
ACS Omega 2025, 10, 19045−19060

remaining compounds. Subsequently, the cells were exposed to 5 μL of JC-1 dye and kept in the dark for 20 min. Following staining, the cells were carefully transferred to falcon tubes and centrifuged at 2000 rpm for 5 min. After centrifugation, the supernatant was removed, and the resulting cell pellets were washed with 1× PBS before being resuspended in 500 μL of 1× PBS. The cell suspensions were then examined using an Amnis Flowsight imaging flow cytometer (Cytek Biosciences) with 10,000 cells analyzed per sample.

2.7. Generation of Reactive Oxygen Species (ROS). Cancer cells were plated in 6-well plates at a density of 1×10^5 cells per well and cultured for 24 h at 37 °C in a 5% CO_2 atmosphere. Subsequently, the cells were exposed to the IC_{50} concentrations of plumbagin, curcumin, or their combination for an additional 24 h. Following treatment, the medium was discarded, and the cells were rinsed twice with 1× PBS to remove any remaining compounds. The cells were then harvested and centrifuged at 2000 rpm, and the resulting pellets were resuspended in 200 μL of 1× PBS. Next, 5 μL of CellRox Green reagent was added to the cell suspension and incubated at 37 °C for 30 min. ROS levels were subsequently quantified using an Amnis Flowsight imaging flow cytometer (Cytek Biosciences) with 10,000 cells evaluated per sample.

2.8. Cell Cycle Analysis. The cells were seeded in 6-well plates at 1×10^5 cells per well and allowed to adhere for 24 h. The cells were then treated with IC_{50} concentrations of plumbagin, curcumin, or their combination for 24 h. After treatment, the cells were collected and the pellets were washed twice with 1× PBS and centrifuged. The pellet was then fixed using 70% ethanol and kept at −20 °C for 30 min to ensure complete fixation. After fixation, the cells were resuspended and washed twice with 1× PBS to eliminate residual ethanol. The cell pellets were resuspended in 200 μL of 1× PBS, stained with 5 μL of PI, and incubated for 30 min. Finally, the stained cells were analyzed using an Amnis Flowsight imaging flow cytometer (Cytek Biosciences) to assess the effect of treatment on the cell cycle progression.

2.9. Assessment of Apoptosis. The cells were cultured in 6-well plates at 1×10^5 cells per well and incubated for 24 h at 37 °C in a 5% CO_2 environment. Following incubation, the cells were exposed to IC_{50} concentrations of plumbagin, curcumin, or their combination for 24 h. Apoptosis was evaluated using an Annexin V-FITC apoptosis kit, following the protocol provided by the manufacturer. The cell pellets were washed twice with 1× PBS and centrifuged. The cells were then resuspended in 100 μL of 1× binding buffer, and 5 μL each of Annexin V-FITC and propidium iodide (PI, final concentration 50 μg/mL) were added to the cell suspension. The mixture was then incubated in the dark for 30 min. Data were acquired using an Amnis Flowsight imaging flow cytometer (Cytek Biosciences).

2.10. DAPI Staining. 4′,6-Diamidino-2-phenylindole (DAPI) is a fluorescent dye that selectively binds to A-T-rich DNA regions, enabling the visualization of nuclear morphology to detect apoptosis. The cells were seeded in 6-well plates at 1×10^5 cells per well and kept at 37 °C in a 5% CO_2 environment for 24 h. Subsequently, the cells were exposed to IC_{50} concentrations of plumbagin, curcumin, or their combination for 24 h. Post-treatment, the cells were stabilized with 4% paraformaldehyde to preserve their structure. The cell membranes were then permeabilized using 0.1% Triton X-100, allowing DAPI to enter the nucleus. The cells were then exposed to a DAPI solution (1 μg/mL) for 5−10 min in the dark to prevent light-induced fading. Apoptotic cells were identified by their condensed, fragmented nuclei, which appeared more luminous and compact under microscopic examination.

2.11. Reverse Transcription Polymerase Chain Reaction (RT-PCR). In 6-well plates, cells were plated at a density of 1×10^5 per well and cultured for 24 h at 37 °C in a 5% CO_2 atmosphere. After this period, the cells were exposed to IC_{50} concentrations of plumbagin, curcumin, or a combination of both. Total RNA was isolated from the treated cells using an RNeasy mini kit (Thermo Fisher), and the RNA quantity was determined using a NanoDrop spectrophotometer (Thermo Fisher). The extracted RNA was converted to cDNA using a cDNA synthesis kit (Thermo Fisher). Quantitative RT-PCR was conducted using RealQ Plus 2X MasterMix Green-without Rox (Amplicon, Denmark), and gene expression was evaluated using primers specific for p53, Bax, and Bcl-2 (Macrogen, Seoul, Korea). A LightCycler 96 real-time PCR system (Roche Applied Science) was used for cDNA amplification. The expression data were standardized against the housekeeping gene (GAPDH), and the relative expression levels of the target genes were determined. The forward and reverse primer used for the p53, Bax, and Bcl-2 genes are listed in Table 1.

2.12. Lipid Peroxidation (LPO) Assay. Cancer cells were cultured in 6-well plates at a density of 1×10 cells per well and incubated for 24 h at 37 °C in a 5% CO_2 environment. Following this period, the cells were exposed to IC_{50} concentrations of plumbagin, curcumin, and their combination. The TBARS method with slight modification, was used to assess lipid peroxidation.[17] The cells were harvested by centrifugation, sonicated in chilled potassium chloride (1.15%), and centrifuged again at 3000*g* for 10 min. A 2 mL volume of TBA reagent (comprising 15% TCA, 0.7% TBA, and 0.25 N HCl) was added to 1 mL of the resulting supernatant. The mixture was then heated to 100 °C for 15 min in a water bath. After cooling, the samples were centrifuged at 1000*g* for 10 min. The absorbance of the supernatant was measured at a 535 nm wavelength.

2.13. Catalase Activity. Cancer cells were seeded in 6-well plates at a density of 1×10^5 cells per well and incubated for 24 h at 37 °C in a 5% CO_2 atmosphere. Subsequently, the cells were treated with IC_{50} concentrations of plumbagin, curcumin, or their combination. The reaction mixture contained phosphate buffer (pH 7.0), 0.08 μmol of H_2O_2, and enzyme protein. Catalase activity was determined by monitoring the reduction in H_2O_2 at 570 nm.[18]

2.14. Superoxide Dismutase (SOD) Activity. Cancer cells were plated in 6-well plates at a density of 1×10^5 cells per well and incubated for 24 h at 37 °C in a 5% CO_2 environment. The cells were then exposed to IC_{50} concentrations of plumbagin, curcumin, or their combination. The reaction mixture consisted of 0.052 M sodium pyrophosphate buffer (pH 8.3), 186 μM PMS, 300 μM NBT, 780 μM NADH, sonicated enzyme, and water.[19] The reaction was initiated by adding NADH and incubating at 37 °C for 90 s. Glacial acetic acid (1.0 mL) was added to stop the reaction, followed by thorough mixing with 4.0 mL of n-butanol. After a 10 min rest period, the mixture was centrifuged and the *n*-butanol layer was collected. A spectrophotometer was used to measure the color intensity of the chromogen in the n-butanol layer at 560 nm, with pure butanol serving as a blank. A control sample of the cell suspension without enzymes was used for comparison.

https://doi.org/10.1021/acsomega.5c01258
ACS Omega 2025, 10, 19045−19060

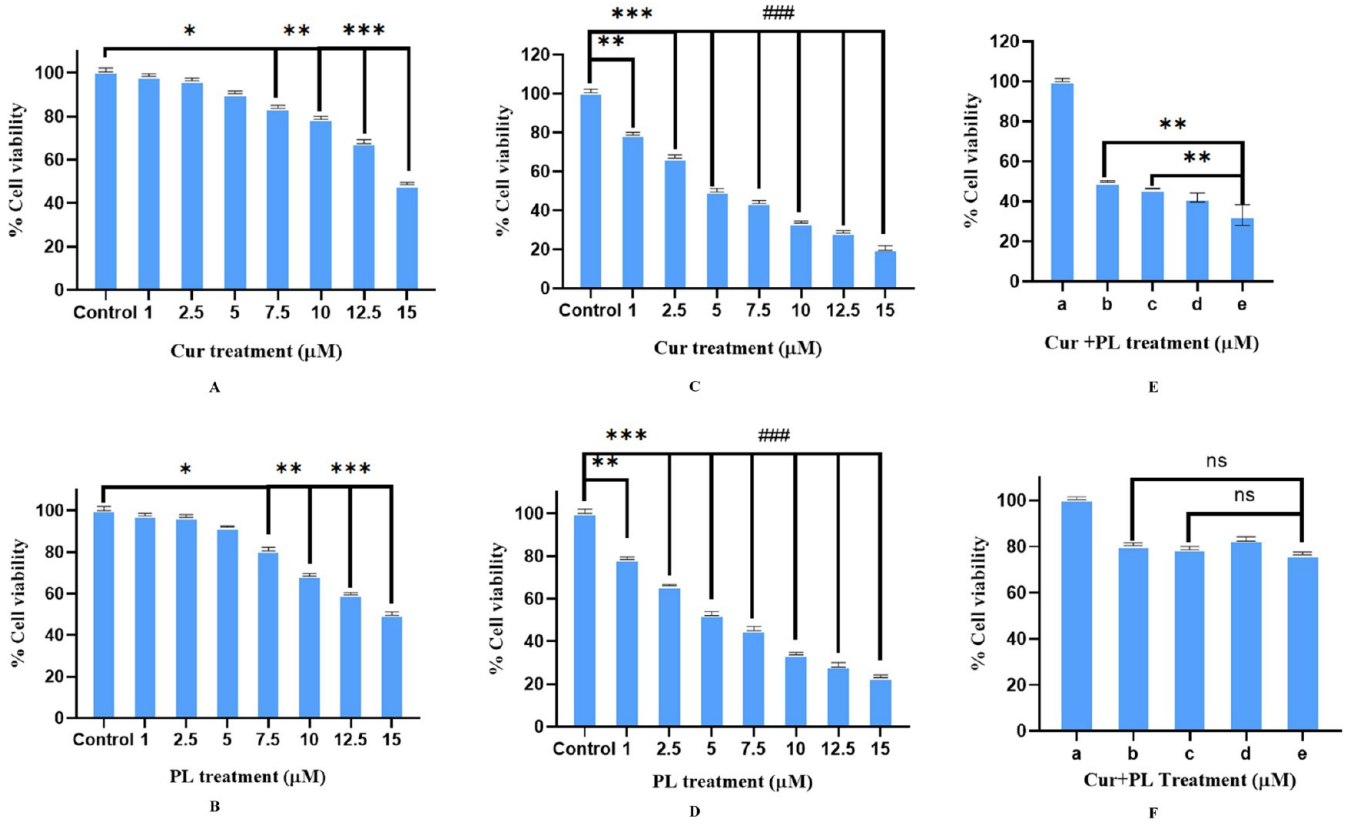

Figure 1. Percentages of cell viability (A: PCS-201-013-Cur treatment B: PCS-201-013-PL treatment, C: HCT-116-Cur treatment, D: HCT-116-PL treatment, E: HCT-116 Cur + PL treatment, and F: PCS-201-013-Cur+PL treatment, where a = control, b = treated with IC_{50} concentration of Cur, c = treated with IC_{50} concentration of PL, and d = treated with IC_{25} concentration of Cur+PL, and e = treated with IC_{50} concentration of Cur +PL).

2.15. Computational Analysis. *2.15.1. Protein and Ligand Preparation.* The three-dimensional structures of the target proteins, p53 (PDB ID: 8DC7), Bcl-2 (PDB ID: 6QGG), and Bax (PDB ID: 8G1T), were retrieved from the Protein Data Bank (https://www.rcsb.org/) on October 1, 2024. The proteins were prepared for molecular docking studies by removing water molecules, heteroatoms, and ligands using the BIOVIA Discovery Studio. The ligands curcumin and plumbagin were obtained from the PubChem database and saved in the SDF format.

2.15.2. Molecular Docking Studies. The docking studies were performed using (PyRx), with an exhaustiveness value of 8 (default setting) to balance computational efficiency and pose prediction accuracy. The grid box center was positioned to cover the entire receptor, ensuring that no binding regions were excluded from the sampling space. To ensure comprehensive sampling of potential binding sites, the entire receptor structure was enclosed within the grid box. The dimensions were carefully selected to encompass the full protein structure, allowing for an unbiased exploration of all possible ligand-binding regions. The specific grid box dimensions for each receptor were as follows:

Bax receptor: grid box size: 50 Å(x) × 55 Å(y) × 49 Å(z)

p53 receptor: grid box size: 84 Å(x) × 79 Å(y) × 101 Å(z)

Bcl-2receptor: grid box size: 54 Å(x) × 48 Å(y) × 66 Å(z)

To assess the synergistic effects of the compounds, each protein receptor was combined with plumbagin to form a single unit by using the PyMOL software. The combined units were then docked with curcumin.

2.16. Statistical Analysis. The data are displayed as the mean ± standard deviation of three independent experiments (n = 3). To perform statistical analysis, GraphPad Prism (version 8.0.2) was used. Dunnett's multiple comparison test was used after one-way analysis of variance (ANOVA) to evaluate the significance of the results. If the p-value was less than 0.05, it was deemed statistically significant. Note: * $p \leq 0.05$, ** $p \leq 0.01$, and *** $p \leq 0.001$.

3. RESULTS

3.1. Cell Viability. Treatment with curcumin or plumbagin alone significantly reduced the cell viability in a dose-dependent manner. The IC_{50} value of curcumin was found to be 7.7 μM, whereas the IC_{50} value of plumbagin was recorded as 7.5 μM (Figure 1C,D). However, the mixture of these compounds further reduced cell viability and the IC_{50} concentration reduced to 6.8 μM (Figure 1E). In addition, the PCS-201-013 cells showed non-significant cytotoxicity up to the IC_{50} concentration of both curcumin and plumbagin; however, a slight decline in cell viability was observed at concentrations higher than the IC_{50} (Figure 1A,B).

The therapeutics index of curcumin and plumbagin was calculated as 2.1 and 2.3, respectively, against noncancerous cell line.

The therapeutic index was calculated as mentioned below:

https://doi.org/10.1021/acsomega.5c01258
ACS Omega 2025, 10, 19045−19060

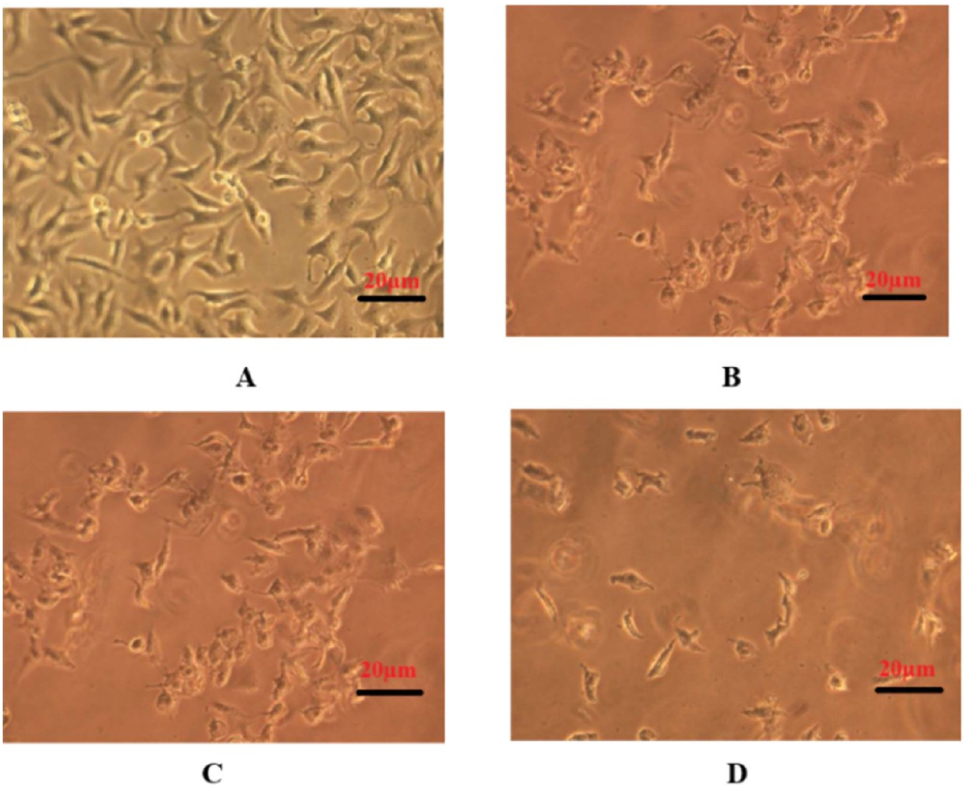

Figure 2. Morphological alteration in HCT-116 cells after 24 h of treatment (A: Untreated control cells, B: Cur-treated cells, C: PL-treated cells, and D: Cur + PL-treated cells).

The IC_{50} for curcumin was 14.5 against the PCS-201-013 cell line.

The combined cytotoxic concentration (IC_{50}) of Cur + PL against HCT-116 was 6.8.

Hence, therapeutic index of curcumin = ED_{50}/TD_{50} (14.5/6.8 = 2.1).

Similarly, the IC_{50} for plumbagin was 16 against the PCS-201-013 cell line.

The combined cytotoxic concentration (IC_{50}) of Cur + PL against HCT-116 was 6.8.

So, therapeutic index of plumbagin = ED_{50}/TD_{50} (16/6.8 = 2.3).

3.2. Morphological Changes. Cancer cells treated with curcumin, plumbagin, or their combination displayed significant morphological changes compared with untreated controls. These alterations include pronounced cellular deformities such as irregular shapes, membrane blebbing, and cellular shrinkage. The treated cells exhibited a marked reduction in size and altered structural integrity, characterized by a reduction in cell-to-cell adhesion and an increase in granularity. These morphological changes indicated cytotoxic effects, suggesting that the studied compound induced cell death, resulting in substantial cellular damage and compromised integrity (Figure 2).

3.3. Scratch Wound Healing Assay. Treatment with curcumin or plumbagin alone significantly inhibited the cell migration. On the other hand, the combined treatment resulted in a substantial reduction in migration compared to the individual compounds, relative to the 0 h time point. The untreated control cells migrated efficiently, covering approximately 55% of the wound area after 24 h. In contrast, cells treated with a combination of curcumin and plumbagin exhibited only 12% migration (Figure 3). This marked inhibition of cell movement underscores the synergistic mechanism of action between these two compounds and suggests the potential of combination therapy for cellular motility disruption, which is a critical factor in cancer progression and metastasis.

3.4. Mitochondrial Membrane Potential ($\Delta\Psi_M$). Mitochondrial membrane potential (MMP) is essential for cellular energy production and the regulator of apoptosis and can have a profound effect on cell survival and death. A significant depolarization of MMP was observed in Cur + PL-treated cells compared to that in the individual compounds as indicated by areas under peak (Figure 4A–D).

3.5. Reactive Oxygen Species (ROS). Treatment with curcumin, plumbagin, or their combination significantly enhanced the production of ROS in HCT-116 cells. As illustrated in Figure 5A–E, ROS levels were markedly increased in cells treated with the combination compared with those treated with individual compounds. Increased ROS production leads to cellular damage and oxidative stress, thereby reinforcing the synergistic effect of curcumin and plumbagin in facilitating cancer cell death via oxidative mechanisms.

3.6. DAPI Staining. DAPI staining showed a stronger fluorescence signal in cells treated with the curcumin and plumbagin combination compared to that with the singlet compound, indicating heightened chromatin condensation (Figure 6A–D). The presence of shrunken nuclei in the treated cells served as a clear indicator of apoptotic cell death, confirming the synergistic effect of curcumin and plumbagin in promoting apoptosis.

https://doi.org/10.1021/acsomega.5c01258
ACS Omega 2025, 10, 19045−19060

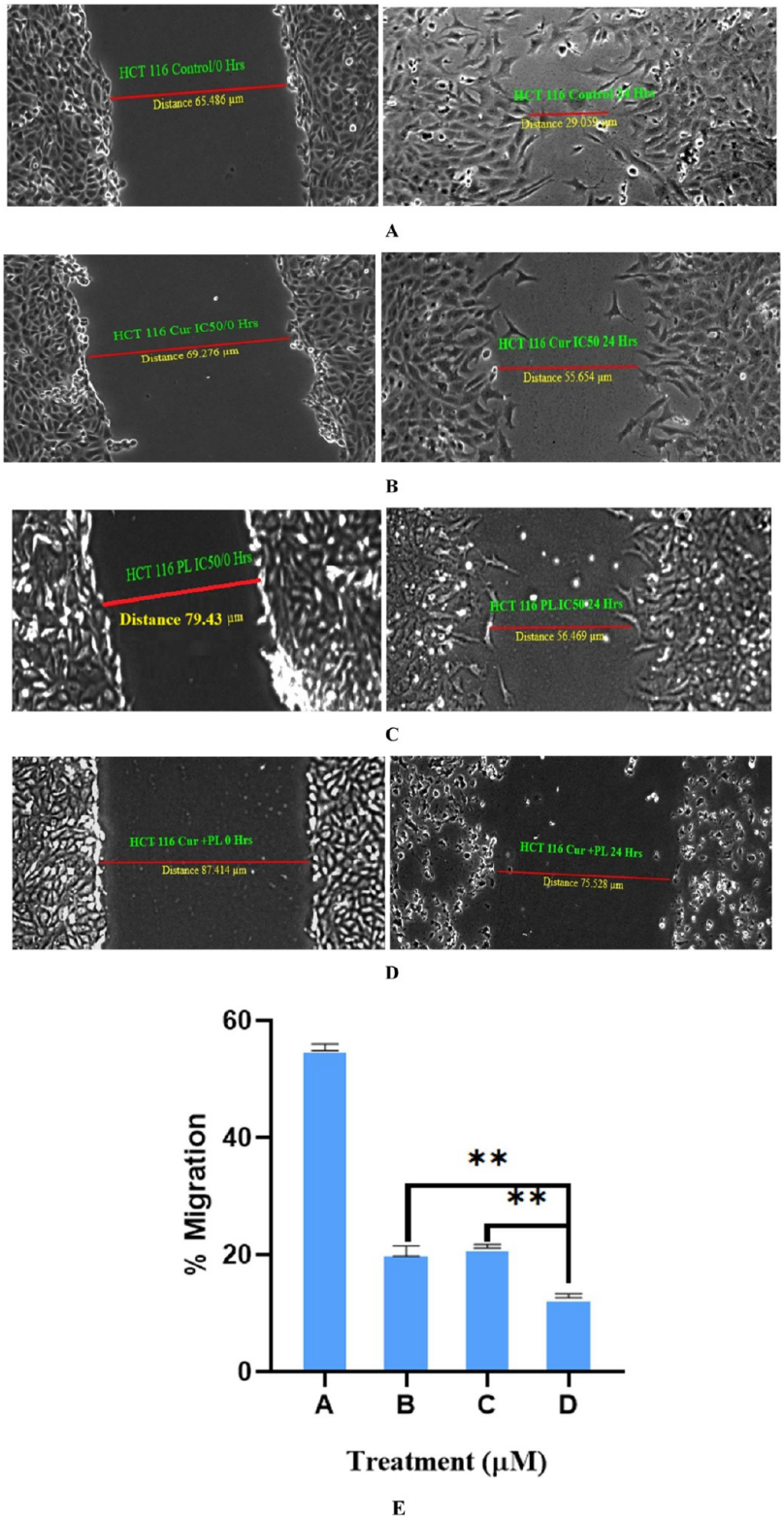

Figure 3. Scratch wound healing assay in HCT-116 cell lines at 0 and 24 h (A: Untreated control cells, B: Cur-treated cells, C: PL-treated cells, and D: Cur + PL-treated cells). E: Percentage migration. Left 0 h; Right, 24 h.

3.7. Catalase Activity Assay. HCT-116 cells treated with a combination of curcumin and plumbagin showed a significant reduction in catalase activity (~40%) compared with the control. This marked decrease in catalase activity suggests that the combined treatment exacerbates oxidative stress by diminishing the capacity of cells to neutralize ROS, thereby reinforcing the synergistic effect of curcumin and plumbagin in promoting oxidative stress and inducing cancer cell death (Figure 7).

3.8. Superoxidase (SOD) Activity Assay. A time-dependent decline in the SOD level was observed in HCT-116 cells treated with curcumin, plumbagin, or their

https://doi.org/10.1021/acsomega.5c01258
ACS Omega 2025, 10, 19045−19060

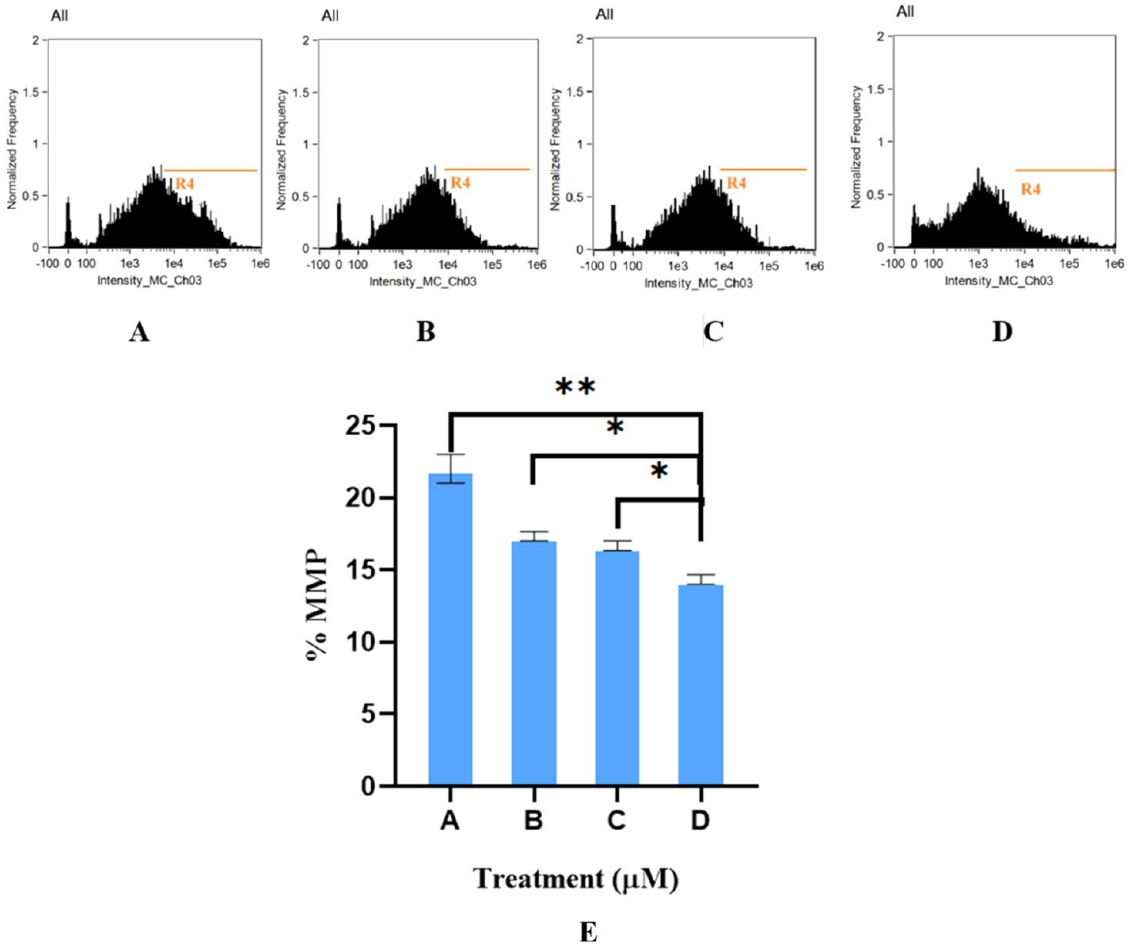

Figure 4. Mitochondrial membrane potential in HCT-116 cells (A: Untreated control cells, B: Cur-treated cells, C: PL-treated cells, and D: Cur + PL-treated cells). E: Percentage change in MMP in response to individual compounds and their combination.

combination. The reduction in the SOD activity began within 2 h of treatment and continued to decline progressively over time. This reduction in SOD activity indicates an increase in oxidative stress within the cells, emphasizing the sustained effect of the treatment on the cellular oxidative balance (Figure 8).

3.10. Lipid Peroxidation (LPO). A moderate increase in LPO was observed following plumbagin or curcumin treatment. However, the combination of Cur + PL treatment led to an increase in LPO of approximately by 42% in the studied cell lines (Figure 9). The increased LPO observed in the combined treatment group may be due to high ROS production, which surpassed cellular defenses and led to significant damage to the lipid membranes. This synergism likely enhances anticancer efficacy because increased oxidative damage adversely affects cancer cell survival.

3.11. Cell Cycle Progression. Cell cycle analysis revealed a variable percentage of cells across various stages of the cell cycle in response to curcumin, plumbagin, or their combination (Figure 10 and Table 2). The percentages of cells in the G2/M phase were 17%, 22%, 34%, and 45% in the control, Cur, PL, and Cur + PL-treated groups, respectively. In contrast, the percentage of cells in the S-phase was markedly diminished in the combined treatment group. Cell cycle arrest in the G2/M phase indicates a synergistic effect of curcumin and plumbagin concurrent exposure.

3.12. Induction of Apoptosis. The percentages of apoptotic cells were 25, 29, and 41% upon treatment with curcumin, plumbagin, and their combination, respectively (Figure 11 and Table 3). These findings indicate a synergistic interaction between curcumin and plumbagin, as the combination treatment notably enhanced the proportion of apoptotic cells compared with that of the control or single compound.

3.13. Gene Expression. RT-PCR data indicated a 4.9-fold increase in Bax and p53 expression in the combined treatment group after 48 h. In contrast, Bcl-2 expression decreased by 3.9-fold in the same treatment group (Table 4).

3.14. Molecular Docking. To investigate the combinatory effects of plumbagin and curcumin, both compounds were docked separately and in combination with three distinct apoptotic proteins: Bax, Bcl-2, and p53 (Figures 12−14). Curcumin demonstrated a binding energy of −7.7, −6.4, and −6 kcal/mol with the Bcl-2, Bax, and p53 proteins, respectively, whereas plumbagin showed binding energies of −6.3, −6, and −6.5 kcal/mol with the same set of proteins. The receptor protein-plumbagin ligand complex was docked with curcumin for a synergistic evaluation. The binding energy of the Bcl-2-plumbagin complex with curcumin was −8 kcal/mol, whereas the Bax-plumbagin complex exhibited a binding energy of −8.4 kcal/mol. Moreover, the p53-plumbagin complex exhibited a binding energy of −6.1 kcal/mol when associated with curcumin (Table 5). The docking results were

https://doi.org/10.1021/acsomega.5c01258
ACS Omega 2025, 10, 19045−19060

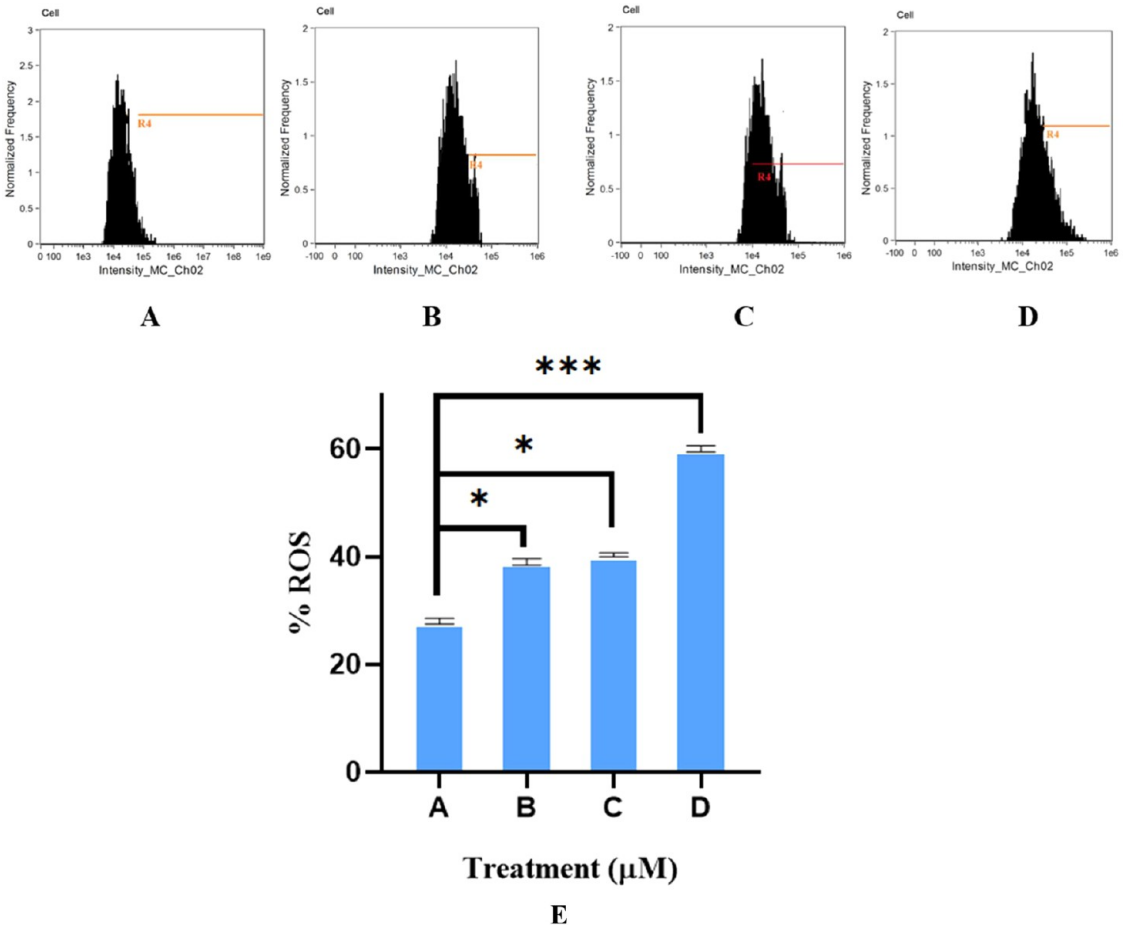

Figure 5. Reactive oxygen species (ROS) production in HCT-116 cells (A: Untreated control cells, B: Cur-treated cells, C: PL-treated cells, and D: Cur + PL-treated cells). E: Percentage change in ROS in response to individual compound and their combination.

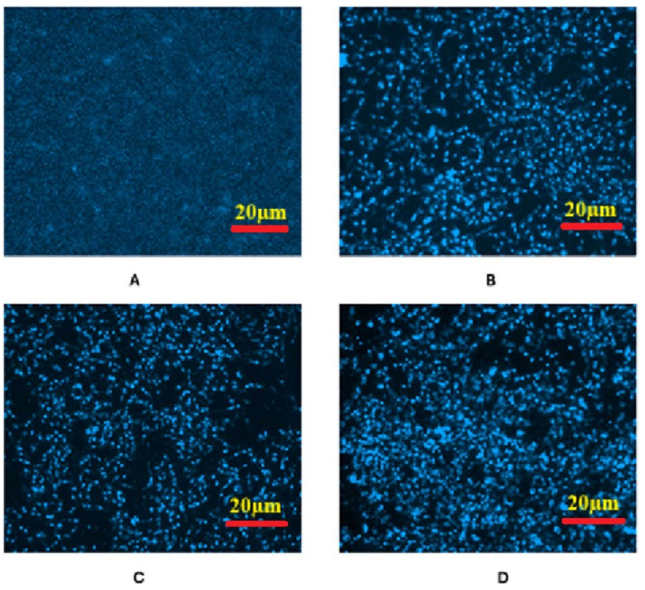

Figure 6. DAPI staining of HCT-116 cells (A: Untreated control cells, B: Cur-treated cells, C: PL-treated cells, and D: Cur + PL-treated cells).

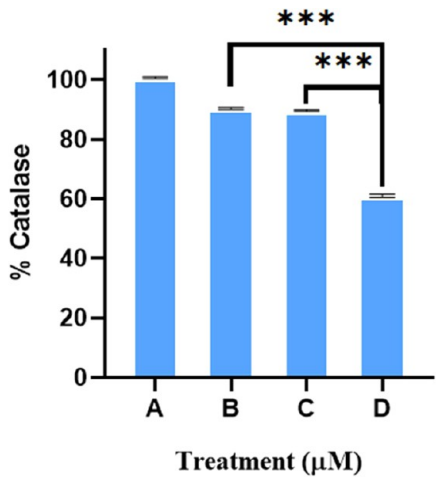

Figure 7. Catalase activity assay of HCT-116 cells (A: Untreated control cells, B: Cur-treated cells, C: PL-treated cells, and D: Cur + PL-treated cells).

validated by two other platforms, namely, "YASARA GLOBAL DOCKING" (included within licensed YASARA STRUCTURE) and "CLICKDOCK", and furthermore by redocking. It is imperative to mention that the results from the aforementioned platforms were found to be in harmony with each other for the studied complexes. Overall, these results showed superior binding affinity for the combination of plumbagin and curcumin compared to those of the individual compounds.

https://doi.org/10.1021/acsomega.5c01258
ACS Omega 2025, 10, 19045−19060

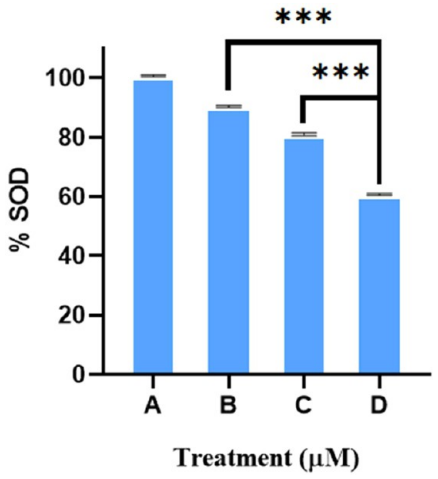

Figure 8. SOD activity assay of HCT-116 cells (A: Untreated control cells, B: Cur-treated cells, C: PL-treated cells, and D: Cur + PL-treated cells).

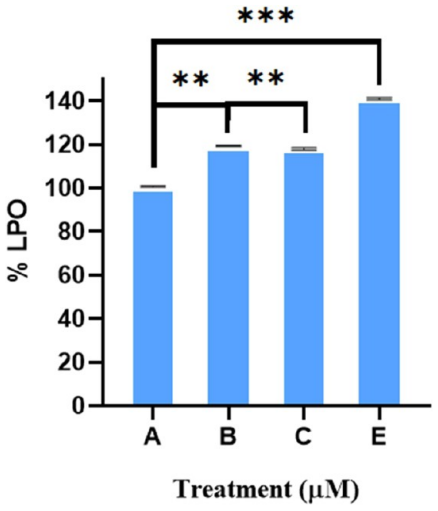

Figure 9. Lipid peroxidation in HCT-116 cells (A: Untreated control cells, B: Cur-treated cells, C: PL-treated cells, and D: Cur + PL-treated cells).

4. DISCUSSION

Chemotherapeutic drugs are used for the treatment of colon cancer because of their strong antitumor effects; however, they can also cause considerable damage to healthy cells, leading to severe side effects including drug resistance.[20] Curcumin and plumbagin as solitary compounds have demonstrated strong anticancer efficacy in a wide range of cancer models. In this study, we observed a significant enhancement in the anticancer potential of curcumin and plumbgin combination, especially against colon cancer cell line (HCT-116). Cell viability assays demonstrated a dose-dependent decrease in cell viability after treatment with curcumin or plumbagin (Figure 1C,D). However, the combined treatment showed superior efficacy compared with the individual compounds, validating their synergistic effect (Figure 1E). This synergistic effect may be due to the activation of complementary mechanisms that simultaneously inhibit several molecular pathways.[16,21] Similar synergistic effects have been reported in the scientific literature when a combination of curcumin or plumbagin was used with other phytoconstituents like resveratrol, quercetin, and epigallocatechin.[22−26] Oxaliplatin, a common colon cancer drug has been reported to inhibit colon cancer cells with IC_{50} concentrations of 38 μM, 46 μM, and 24 μM, against HCT-116, HCT-8, and HT-29 cells, respectively,[27] which is comparatively very high in comparison of combined curcumin and plumbagin IC_{50} concentration. One study reported the reduced cell viability and inhibiting proliferation by standard therapeutics like 5-fluorouracil (5-FU) against colon cancer cells (HCT-116, HCT-115, and CO-115) and recorded its IC_{50} in the range of 100 μM.[28] Similarly, another study observed induction in apoptosis by 5-FU with an IC_{50} concentration of 50 μM in colon cells.[29]

Cancer cell morphological changes associated with apoptosis include cell shrinkage, nuclear condensation, and the formation of apoptotic bodies, which are indicative of programmed cell death.[30,31] The scratch assay revealed that curcumin and plumbagin significantly inhibited cell migration, indicating notable antimigratory potential. This effect was particularly pronounced in the combined treatment group (Figure 3D). This is consistent with other studies where curcumin or plumbagin have been reported to reduce cancer cell metastasis through the inhibition of various pathways.[32−34]

The MMP assay showed considerable depolarization of the mitochondrial membrane in response to Cur and PL treatment, suggesting the activation of the intrinsic apoptotic pathway (Figure 4). This might be because of curcumin's ability to induce plumbagin's capacity to produce ROS, may impair mitochondrial function.[35−37] This was also confirmed by ROS estimation, which demonstrated a significant increase in ROS generation when Cur and PL were treated in combination (Figure 5). The enhanced oxidative damage and apoptosis in response to excessive ROS production can overwhelm the antioxidant defenses of cancer cells.[38,39] Increased ROS levels also lead to DNA damage, oxidative stress, and MMP disruption, all of these can induce apoptosis.[40,41]

DAPI staining and membrane integrity assessments also revealed significant nuclear changes, including chromatin condensation and fragmentation of nuclear material, particularly in cells treated with both curcumin and plumbagin (Figure 6). Nuclear alterations are the defining characteristics of apoptosis, as confirmed by DAPI/PI staining, which indicates late apoptotic stages.[42,43] Superoxide dismutase and catalase are two important antioxidant enzymes that reduce ROS to protect cells from oxidative damage.[44,45] The reduced catalase and SOD levels in our study indicate that curcumin and plumbagin induce significant oxidative stress through ROS-mediated cellular apoptosis. Elevated LPO, an indicator of oxidative damage, further substantiated that oxidative stress is pivotal for the anticancer actions of curcumin and plumbagin combination (Figure 9). Lipid peroxidation occurs when ROS target polyunsaturated fatty acids within the cell membrane.[46,47]

This pro-oxidant mechanism is in line with the ability of curcumin and plumbagin to disrupt redox balance and trigger cell death.[48−50] A well-known chemotherapeutic drug (cisplatin) has been reported to induce oxidative stress via enhanced production of ROS in colon cancer cells, similar to the combined treatment of curcumin and plumbagin.[51]

The cell cycle study showed that the combination of curcumin and plumbagin was responsible for cell cycle arrest in the G2/M phase. The cell cycle arrest at the G2/M phase is an indication of DNA fragmentation and apoptotic cell death.[52,53]

https://doi.org/10.1021/acsomega.5c01258
ACS Omega 2025, 10, 19045−19060

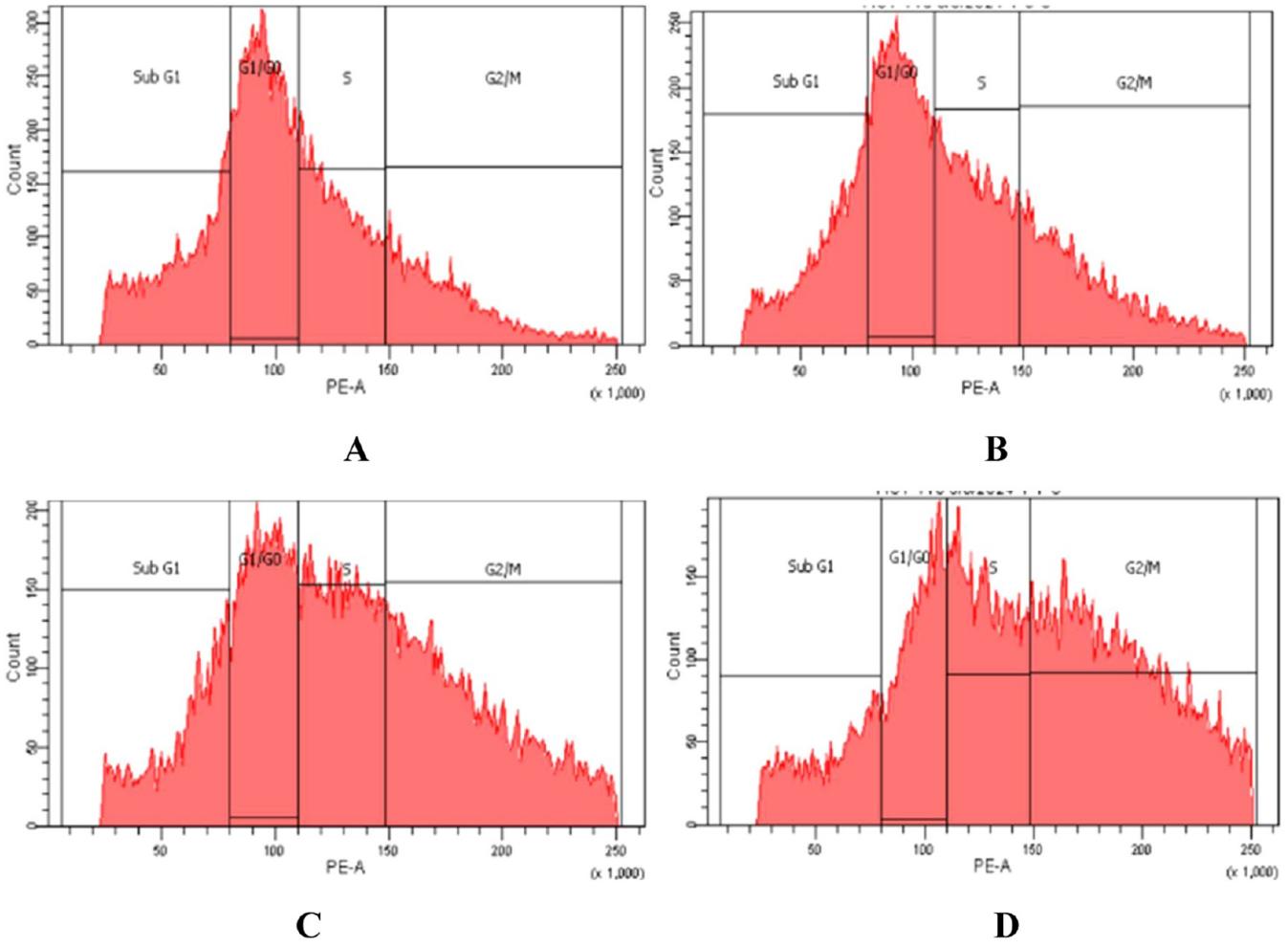

Figure 10. Cell cycle analysis by flow cytometry (A: Untreated control cells, B: Cur-treated cells, C: PL-treated cells, and D: Cur + PL-treated cells).

Table 2. Cell Percentages at Different Phases of Cell Cycle

phases	control (%)	Cur-treated	PL-treated	Cur + PL-treated
Sub-G1	22	20	15	11
G1/Go	35	31	23	17
S	24	25	26	25
G2/M	17	22	34	45

Oxaliplatin completely blocks the G2/M transition, inducing cell cycle arrest at the G2/M phase in HCT-116 cells.[54] The observed increase in apoptosis correlates with the activation of the internal and extrinsic apoptotic pathways, as demonstrated by a decrease in MMP and elevated ROS.[55,56] Colon cancer cells treated with celecoxib have been noted to suppress cell growth, which is linked to reduced proliferation and increased apoptosis.[57]

The expression patterns of p53, Bax, and Bcl-2 were consistent with earlier reports indicating the effect of curcumin and plumbagin on these apoptotic regulators.[58,59] The anti-inflammatory and antioxidant properties of curcumin, along with the pro-oxidant activity of plumbagin, may have detrimental effects on cancer cells by interfering with various cellular processes, such as mitochondrial function, ROS production, and cell cycle progression. This synergy corroborates the increasing evidence that supports combination therapies for cancer treatment that affect multiple molecular pathways.

Curcumin and crocin synergistically reduced colon cancer cell viability, induced apoptosis, modulated apoptosis-related gene expression, increased sub-G1 cell cycle arrest, triggered autophagy, and reduced clonogenicity.[60] The combination of curcumin and 5-FU has also been reported to synergistically reduce SW620 cell proliferation and migration, induce apoptosis, extend survival of immunodeficient mice, inhibit protein kinase R-like ER kinase (PERK) signaling, and downregulate L1 expression.[61] Similarly, the combination of zoledronic acid (ZA) and plumbagin has been noted to synergistically suppress MDA-MB-231SArfp breast cancer cells by inhibiting ZA-induced Notch-1 activation, reducing Bcl-2 expression, and inducing apoptosis.[62] One study reported that plumbagin and celecoxib synergistically kill melanoma cells by inhibiting COX-2 and STAT3 pathways, reducing proliferation, inducing apoptosis, and impairing vascular development. This combination has also been reported to reduce tumor growth by 63% in a xenograft model with minimal toxicity, highlighting the potential of this combination for overcoming melanoma drug resistance.[63]

Our molecular docking data also confirmed the *in vitro* data and showed an enhanced binding energy of the tirad complex, especially for Cur + PL + Bax/Bcl-2. Curcumin and plumbagin have demonstrated promising synergistic anticancer effects, but

https://doi.org/10.1021/acsomega.5c01258
ACS Omega 2025, 10, 19045−19060

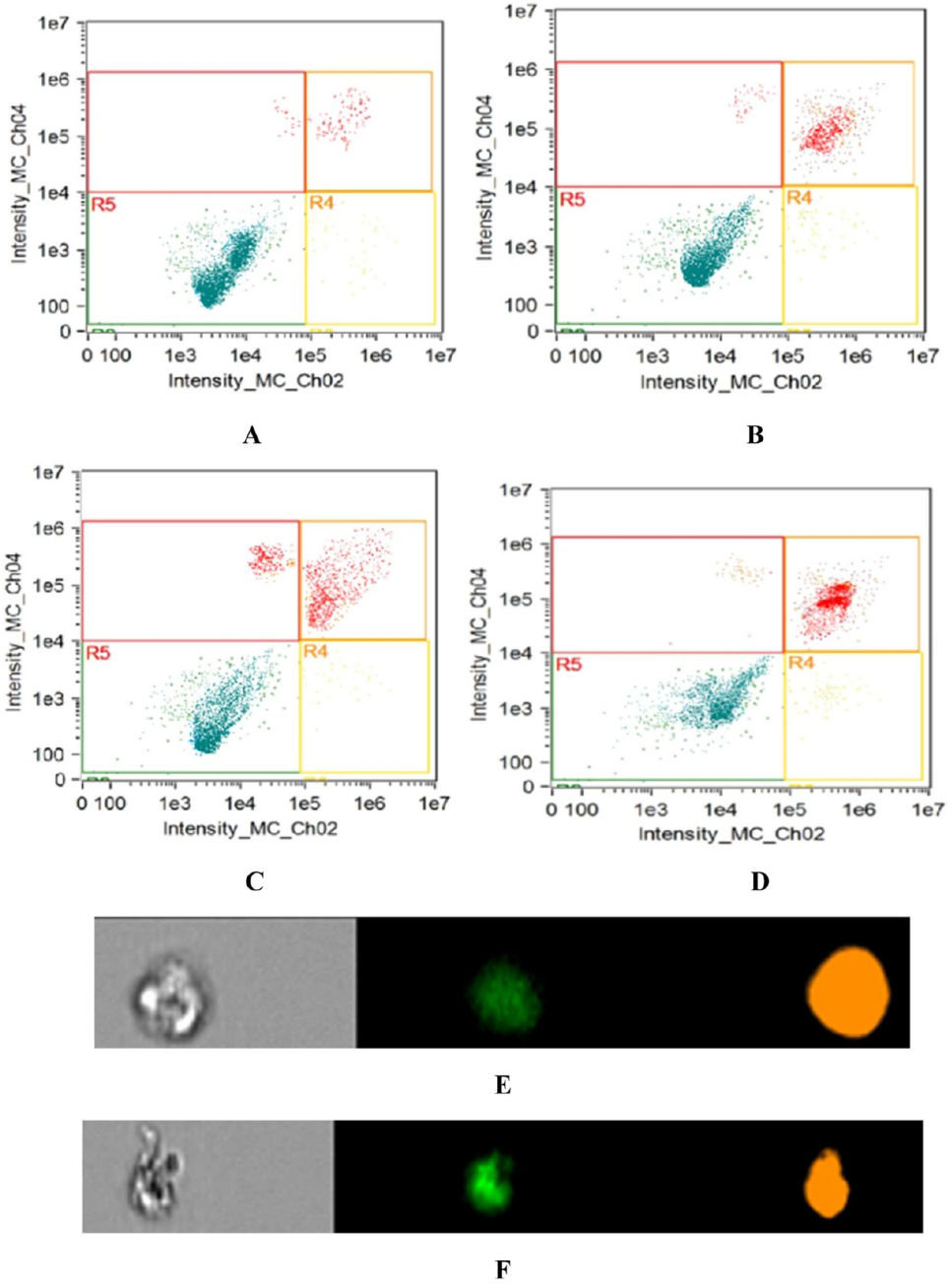

Figure 11. Induction of apoptosis by flow cytometry (A: Untreated control cells, B: Cur-treated cells, C: PL-treated cells, and D: Cur + PL-treated cells). (E, F): Change in the shapes of control and combined treated cells, respectively. (Note: In the quadrant, R5 is total viable cells, R4 is early apoptotic cells, above R4 is late apoptotic cells, and above R5 is necrotic cells. In addition, Annexin V-positive/PI-negative (early apoptosis), Annexin V-positive/PI-positive (late apoptosis), and Annexin V-negative/PI-negative (live cells).

Table 3. Cell Percentages at Different Apoptotic Events

events	control (%)	Cur-treated	PL-treated	Cur + PL-treated
live cells	91	69	63	49
total apoptotic cells	5	25	29	41
necrotic cells	2	4	5	9

Table 4. Expression Pattern of Bcl-2 (A), Bax (B), and p53 (C) Genes in HCT-116 Cells

gene names	Cur-treated	PL-treated	Cur + PL-treated	time (h)
Bcl-2 (fold-decrease)	1.17	2.7	3.5	24
	1.9	2.8	3.9	48
Bax (fold-increase)	2.03	2.9	4.7	24
	2.5	3.4	4.9	48
p53 (fold-increase)	1.3	1.4	4.1	24
	1.7	1.9	4.9	48

their clinical applications are hindered by poor bioavailability and stability. Despite curcumin's well-known anticancer properties, it suffers from rapid metabolism and poor absorption, which significantly reduce its therapeutic effectiveness.[64] Similarly, plumbagin's low solubility in water limits its absorption and efficacy.[33] To address these challenges, various nanoparticle-based delivery platforms have been explored,

https://doi.org/10.1021/acsomega.5c01258
ACS Omega 2025, 10, 19045−19060

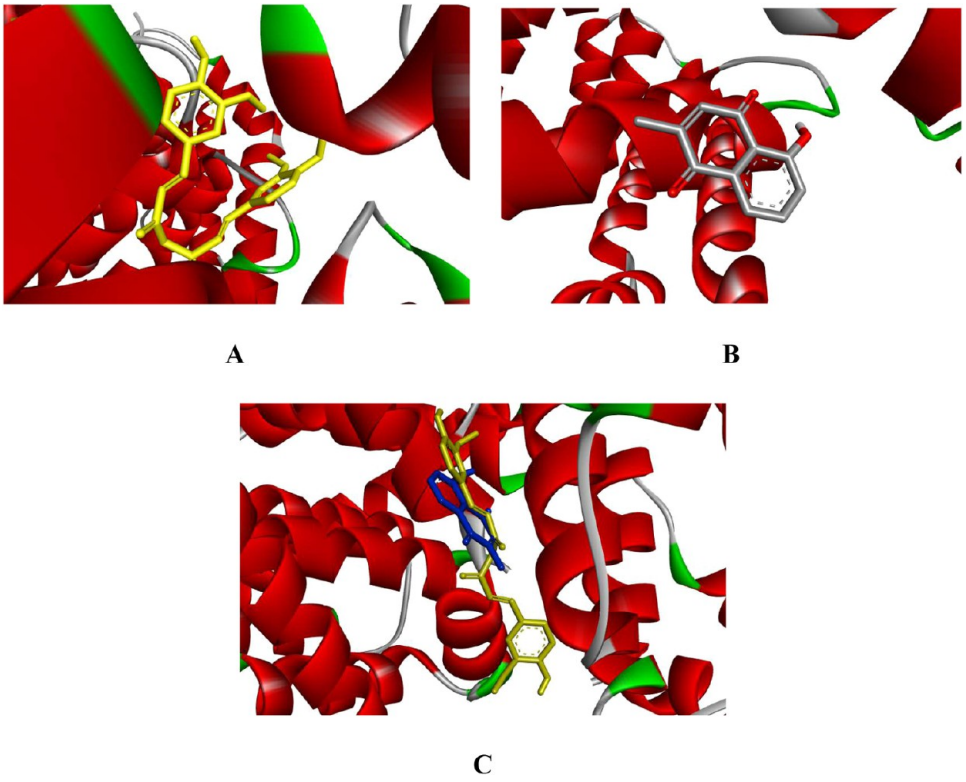

Figure 12. Molecular docking of (A) curcumin, (B) plumbagin, and (C) Cur + PL to Bax protein.

which improved their solubility, stability, and provided targeted delivery to tumor sites.[65,66] Additionally, codelivery systems combining these compounds with other therapeutic agents could further improve therapeutic outcomes by enhancing cellular uptake and reducing systemic toxicity.[25,67] These strategies are essential for overcoming bioavailability issues and increasing the clinical potential of curcumin and plumbagin as effective cancer therapies.

5. STUDY LIMITATIONS

Although results are encouraging, this study has certain limitations that need to be considered during the interpretation of the data. This study was carried out on a single cancer cell line, i.e., HCT-116. We could have also used ROS scavengers to prove an oxidative-stress-induced mechanism of action by the curcumin and plumbagin combination. The protein expression level of anti/apoptotic genes could not be performed in this study due to some technical issues at our disposal. In addition, the lack of long-term toxicity data and comprehensive validation of the obtained data in a suitable xenograft model is required.

6. CONCLUSION AND FUTURE DIRECTIONS

The combination of curcumin and plumbagin demonstrated potent anticancer effects against HCT-116 cells by modulating MMP, increasing ROS production, inducing G2/M cell cycle arrest, and promoting apoptosis through Bcl-2 downregulation and upregulation of p53 and Bax. This led to compromised membrane integrity, increased LPO, and reduced antioxidant enzyme activities. Given these promising *in vitro* results, further *in vivo* validation is necessary to assess efficacy and safety of this combination in a corresponding xenograft model. The clinical applicability of this combination, especially against colon cancer, could be significant, alongside existing small-molecule therapies. For instance, combining these natural compounds with conventional chemotherapeutic agents, like 5-fluorouracil (5-FU) or oxaliplatin, could enhance the therapeutic response in colon cancer patients, potentially overcoming drug resistance and improving treatment outcomes. Additionally, their synergistic effects might be leveraged in combination with targeted therapies, such as epidermal growth factor receptor (EGFR) inhibitors or immune checkpoint inhibitors, to improve the efficacy of treatments in advanced-stage cancer patients. Further clinical exploration is also needed to determine optimal dosing, delivery methods (e.g., nanoparticle formulations), and safety profiles for these combinations, advancing them toward possible clinical use.

■ ASSOCIATED CONTENT

Data Availability Statement

The data used to support the findings of this study are available from the corresponding author upon reasonable request.

■ AUTHOR INFORMATION

Corresponding Authors

Ajoy Kumer − *Department of Chemistry, College of Arts and Sciences, International University of Business Agriculture & Technology (IUBAT), Dhaka 1230, Bangladesh;* orcid.org/0000-0001-5136-6166; Email: kumarajoy.cu@gmail.com

Shams Tabrez − *King Fahd Medical Research Center and Department of Medical Laboratory Sciences, Faculty of Applied Medical Sciences, King Abdulaziz University, Jeddah 21589, Saudi Arabia;* orcid.org/0000-0003-4550-415X; Email: shamstabrez1@gmail.com, stabrez@kau.edu.sa

https://doi.org/10.1021/acsomega.5c01258
ACS Omega 2025, 10, 19045−19060

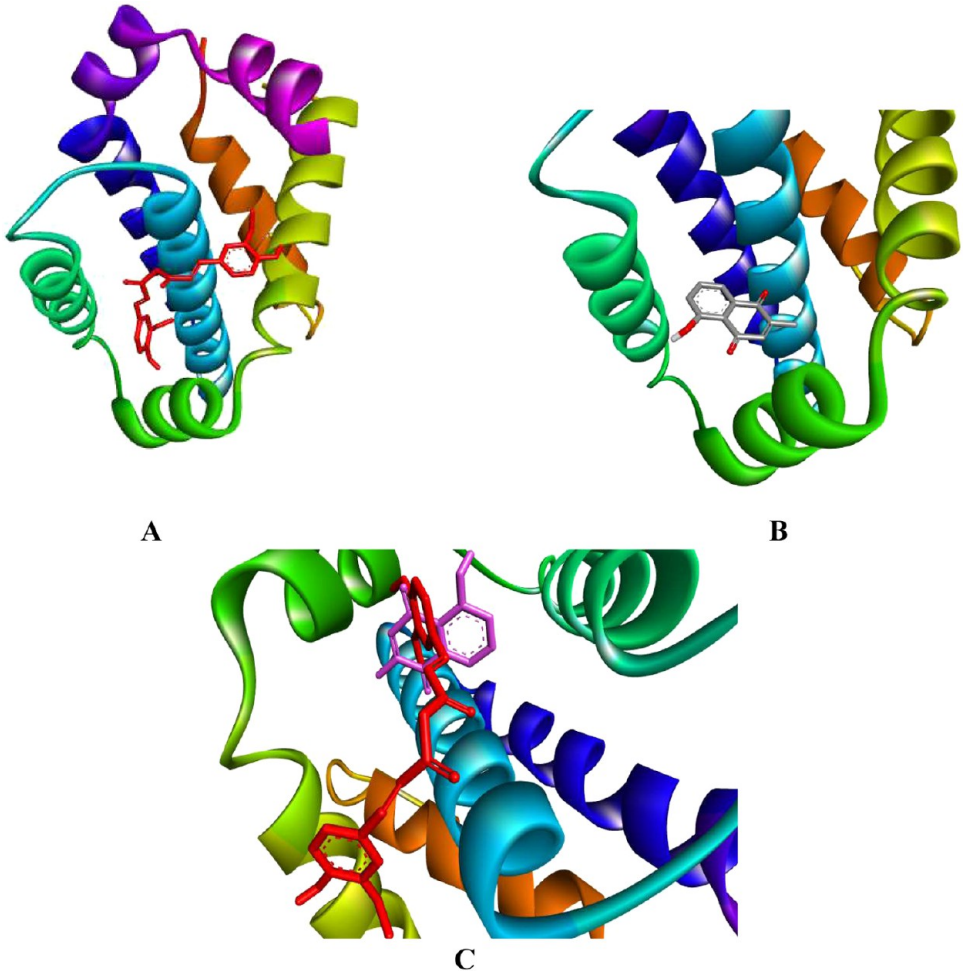

Figure 13. Molecular docking of (A) curcumin, (B) plumbagin, and (C) Cur + PL to the Bcl-2 protein.

Authors

Iftikhar Ahmad − *Department of Biochemistry, Faculty of Science, King Abdulaziz University, Jeddah 21589, Saudi Arabia; King Fahd Medical Research Center, King Abdulaziz University, Jeddah 21589, Saudi Arabia*

Sameer Ahmad − *King Fahd Medical Research Center, King Abdulaziz University, Jeddah 21589, Saudi Arabia; Department of Biological Sciences, Faculty of Science, King Abdulaziz University, Jeddah 21589, Saudi Arabia*

Md Abdus Samad − *Department of Biochemistry, Faculty of Science, King Abdulaziz University, Jeddah 21589, Saudi Arabia; King Fahd Medical Research Center, King Abdulaziz University, Jeddah 21589, Saudi Arabia*

Ahmed Mohammed Adam − *Department of Biochemistry, Faculty of Science, King Abdulaziz University, Jeddah 21589, Saudi Arabia*

Torki A. Zughaibi − *King Fahd Medical Research Center and Department of Medical Laboratory Sciences, Faculty of Applied Medical Sciences, King Abdulaziz University, Jeddah 21589, Saudi Arabia*

Mahmoud Alhosin − *Department of Biochemistry, Faculty of Science, King Abdulaziz University, Jeddah 21589, Saudi Arabia*

Shazi Shakil − *Department of Medical Laboratory Sciences, Faculty of Applied Medical Sciences and Institute of Genomic Medicine Sciences, King Abdulaziz University, Jeddah 21589, Saudi Arabia*

Mohd Shahnawaz Khan − *Protein Research Chair, Department of Biochemistry, College of Science, King Saud University, Riyadh 11451, Saudi Arabia;* orcid.org/0000-0002-4599-5924

Ahdab A. Alsaieedi − *King Fahd Medical Research Center and Department of Medical Laboratory Sciences, Faculty of Applied Medical Sciences, King Abdulaziz University, Jeddah 21589, Saudi Arabia*

Complete contact information is available at: https://pubs.acs.org/10.1021/acsomega.5c01258

Author Contributions

I.A., S.A.: Data curation, investigation, methodology, writing—original draft; M.A., S.S.: Formal analysis, methodology, software, visualization, writing—original draft; A.M.A.: Investigation, methodology, visualization, software, writing—original draft; T.A.Z., M.A., M.S., A.A.A., A.K., S.T.: Conceptualization, formal analysis, resources, supervision, validation, writing—review and editing.

Notes

The authors declare no competing financial interest.

Consent to publish All authors have given their consent to publish this article.

https://doi.org/10.1021/acsomega.5c01258
ACS Omega 2025, 10, 19045−19060

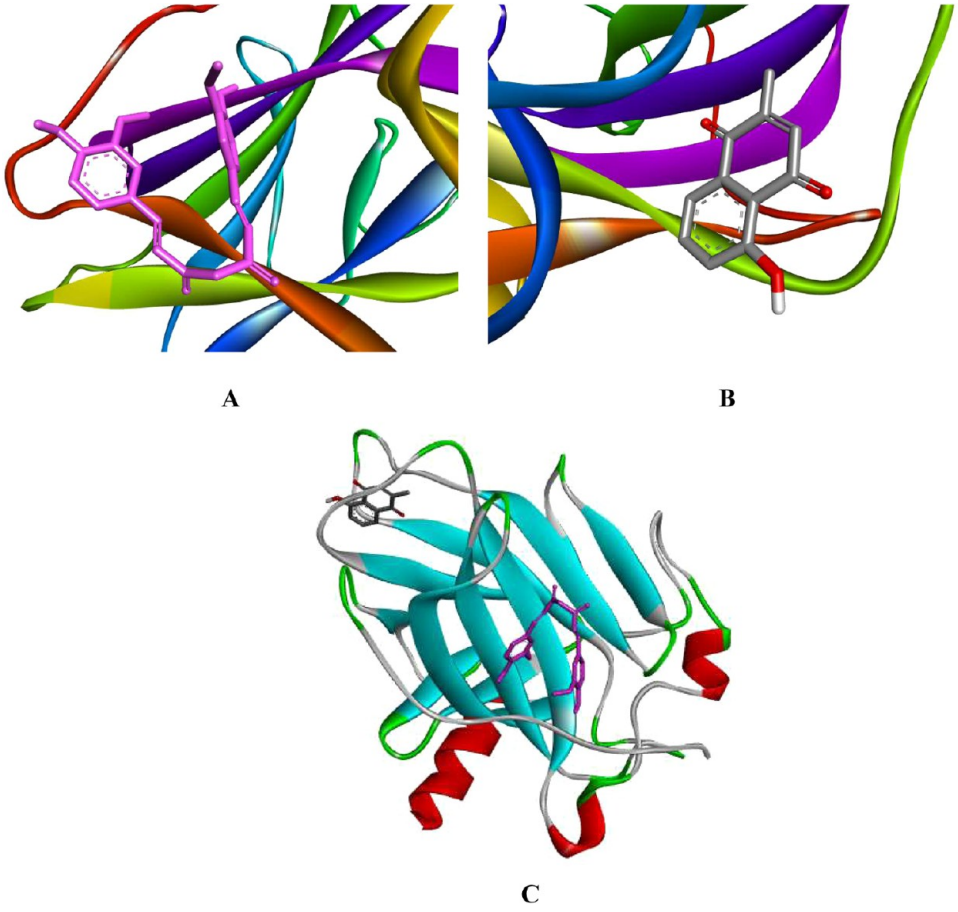

Figure 14. Molecular docking of (A) curcumin, (B) plumbagin, and (C) Cur + PL to p53 protein.

Table 5. Binding Energy (ΔG) of Plumbagin and Curcumin Sequentially Docked with the Bcl-2, Bax, and p53 Proteins

targets	ligand	docking complex	ΔG (kcal/mol)	interacting residues
Bcl-2	Curcumin	Bcl2-Cur	−7.7	ASP111, VAL148, ALA100, ALA149, TYR108, TYR202, PHE104, PHE198
Bcl-2	Plumbagin	Bcl2-PL	−6.3	LUE137, VAL133, ALA149, PHE153, MET115
Bcl2-plumbagin complex	Curcumin	Bcl2-PL-Cur	−8	PHE198, PHE104, ALA100, VAL148, ARG146, ASP111, TYR202, MET115
Bax	Curcumin	Bax-Cur	−6.4	VAL(G121), ARG(C94), LYS(E119), LYS(E123), ASP(C86) SER(C87)
Bax	Plumbagin	Bax-PL	−6	ARG(B94), PHE(B93), ALA(B97), SER(E72)
Bax-plumbagin complex	Curcumin	Bax-PL-Cur	−8.4	GLU(E69), ARG(B94) ARG(B89), ALA(C97) PHE(B93), ALA(B97) ASP(B98)
p53	Plumbagin	p53-PL	−6.5	THR150, PRO222, PRO151, CYS220, THR230, VAL147, PRO223
p53	Curcumin	p53-Cur	−6.	SER269, ASN131, TYR126, LEU111, GLY112, HIS115, ARG110, ASP268, PHE113
p53-plumbagin complex	Curcumin	p53-PL-Cur	−6.1	THR211, PRO98, ILE254, MET160, SER99, ARG267

■ ACKNOWLEDGMENTS

This work was supported by Institutional Fund Projects under grant no [IFPRC-161-290-2020]. Therefore, the authors gratefully acknowledge technical and financial support from the Ministry of Education and King Abdulaziz University, Jeddah, Saudi Arabia.

■ LIST OF ABBREVIATIONS

ATCC:American Type Culture Collection
CRC:colorectal cancer
Cur:curcumin
DAPI:4′,6-diamidino-2-phenylindole
DMSO:dimethyl sulfoxide
PL:plumbagin
MMP:mitochondrial membrane potential
ROS:reactive oxygen species
PMS:phenazine methosulfate
PI:propidium iodide
NBT:nitroblue tetrazolium
RT-PCR:reverse transcription polymerase chain reaction
TBARS:thiobarbituric acid-reactive substances
TBA:thiobarbituric acid

https://doi.org/10.1021/acsomega.5c01258
ACS Omega 2025, 10, 19045−19060

SOD:superoxide dismutase

REFERENCES

(1) Marcellinaro, R.; Spoletini, D.; Grieco, M.; et al. Colorectal Cancer: Current Updates and Future Perspectives. *J. Clin. Med.* **2024**, *13* (1), 40.

(2) Amintas, S.; Dupin, C.; Boutin, J.; et al. Bioactive food components for colorectal cancer prevention and treatment: A good match. *Crit. Rev. Food Sci. Nutr.* **2023**, *63* (23), 6615−6629.

(3) Roshandel, G.; Ghasemi-Kebria, F.; Malekzadeh, R. Colorectal Cancer: Epidemiology, Risk Factors, and Prevention. *Cancers* **2024**, *16* (8), No. 1530, DOI: 10.3390/cancers16081530.

(4) Adigun, A. O.; Adebile, T. M.; Okoye, C.; et al. Causes and Prevention of Early-Onset Colorectal Cancer. *Cureus* **2023**, *15* (9), No. e45095.

(5) Das, S.; Babu, A.; Medha, T.; et al. Molecular mechanisms augmenting resistance to current therapies in clinics among cervical cancer patients. *Med. Oncol.* **2023**, *40* (5), 149.

(6) Andreani, T.; Cheng, R.; Elbadri, K.; et al. Natural compounds-based nanomedicines for cancer treatment: Future directions and challenges. *Drug Delivery Transl. Res.* **2024**, *14* (10), 2845−2916.

(7) Mohd, S.; et al. Leveraging AI and Natural Compounds: Innovative Approaches in the Diagnosis and Treatment of Hepatocellular Carcinoma. *Curr. Pharm. Des.* **2025**, *31*, 1−11.

(8) Cirmi, S.; Maugeri, A.; Micali, A.; et al. Cadmium-Induced Kidney Injury in Mice Is Counteracted by a Flavonoid-Rich Extract of Bergamot Juice, Alone or in Association with Curcumin and Resveratrol, via the Enhancement of Different Defense Mechanisms. *Biomedicines* **2021**, *9* (12), 1797.

(9) Kunnumakkara, A. B.; Hegde, M.; Parama, D.; et al. Role of Turmeric and Curcumin in Prevention and Treatment of Chronic Diseases: Lessons Learned from Clinical Trials. *ACS Pharmacol. Transl. Sci.* **2023**, *6* (4), 447−518.

(10) Tabanelli, R.; Brogi, S.; Calderone, V. Improving Curcumin Bioavailability: Current Strategies and Future Perspectives. *Pharmaceutics* **2021**, *13* (10), No. 1715, DOI: 10.3390/pharmaceutics13101715.

(11) Taneja, N.; Alam, A.; Patnaik, R.; et al. Exploring Plumbago Zeylanica Linn's Anticancer Potential: In Vitro Phytochemical Analysis. *J. Indian Acad. Oral Med. Radiol.* **2024**, *36* (2), 126−131.

(12) Thakor, N.; Janathia, B. Plumbagin: A Potential Candidate for Future Research and Development. *Curr. Pharm. Biotechnol* **2022**, *23* (15), 1800−1812.

(13) Mukherjee, S.; Sawant, A. V.; Prassanawar, S. S.; et al. Copper-Plumbagin Complex Produces Potent Anticancer Effects by Depolymerizing Microtubules and Inducing Reactive Oxygen Species and DNA Damage. *ACS Omega* **2023**, *8* (3), 3221−3235.

(14) Chauhan, S.; Rai, S.; Huddar, V. G. A Review on Clinical and Experimental Studies on Ayurveda and Leukemia. *Med. J. Dr. D.Y. Patil Univ.* **2022**, *15* (2), 158−174.

(15) Shu, J.; Wang, K.; Zhao, D.; et al. Plumbagin induces apoptosis, cell cycle arrest, and inhibits protein synthesis in LoVo colon cancer cells: A proteomic analysis. *Chem. Biol. Drug Des* **2023**, *102* (5), 1075−1084.

(16) Ahmad, I.; Hoque, M.; Alam, S. S. M.; et al. Curcumin and Plumbagin Synergistically Target the PI3K/Akt/mTOR Pathway: A Prospective Role in Cancer Treatment. *Int. J. Mol. Sci.* **2023**, *24* (7), 6651.

(17) Tabrez, S.; Ahmad, M. Some enzymatic/nonenzymatic antioxidants as potential stress biomarkers of trichloroethylene, heavy metal mixture, and ethyl alcohol in rat tissues. *Environ. Toxicol.* **2011**, *26* (2), 207−216.

(18) Tabrez, S.; Ahmad, M. Effect of wastewater intake on antioxidant and marker enzymes of tissue damage in rat tissues: implications for the use of biochemical markers. *Food Chem. Toxicol.* **2009**, *47* (10), 2465−2478.

(19) Tabrez, S.; Ahmad, M. Components of antioxidative system in Allium cepa as the toxicity monitor of trichloroethylene (TCE). *Toxicol. Environ. Chem.* **2011**, *93* (1), 73−84.

(20) Tong, Q.; Wu, Z. Curcumin inhibits colon cancer malignant progression and promotes T cell killing by regulating miR-206 expression. *Clin. Anat.* **2024**, *37* (1), 2−11.

(21) Panda, S. S.; Biswal, B. K. The phytochemical plumbagin: mechanism behind its "pleiotropic" nature and potential as an anticancer treatment. *Arch. Toxicol.* **2024**, *98*, No. 3585, DOI: 10.1007/s00204-024-03861-9.

(22) Piwowarczyk, L.; Stawny, M.; Mlynarczyk, D. T.; et al. Role of Curcumin and (−)-Epigallocatechin-3-O-Gallate in Bladder Cancer Treatment: A Review. *Cancers* **2020**, *12* (7), 1801.

(23) Cecerska-Heryć, E.; Wiśniewska, Z.; Serwin, N.; et al. Can Compounds of Natural Origin Be Important in Chemoprevention? Anticancer Properties of Quercetin, Resveratrol, and Curcumin—A Comprehensive Review. *Int. J. Mol. Sci.* **2024**, *25* (8), 4505.

(24) Gowda, R.; Sharma, A.; Robertson, G. P. Synergistic inhibitory effects of Celecoxib and Plumbagin on melanoma tumor growth. *Cancer Lett.* **2017**, *385*, 243−250.

(25) Cao, C.; Li, Y.; Shi, F.; et al. Nano co-delivery of doxorubicin and plumbagin achieves synergistic chemotherapy of hepatocellular carcinoma. *Int. J. Pharm.* **2024**, *661*, No. 124424.

(26) Zhang, Z.; Li, M.; Zhang, X.; et al. Novel Strategies for Tumor Treatment: Harnessing ROS-Inducing Active Ingredients from Traditional Chinese Medicine Through Multifunctional Nano-formulations. *Int. J. Nanomed.* **2024**, *19*, 9659−9688.

(27) Guichard, S.; Arnould, S.; Hennebelle, I.; et al. Combination of oxaliplatin and irinotecan on human colon cancer cell lines: activity in vitro and in vivo. *Anti-Cancer Drugs* **2001**, *12* (9), 741−751.

(28) Xavier, C. P. R.; Lima, C. F.; Rohde, M.; et al. Quercetin enhances 5-fluorouracil-induced apoptosis in MSI colorectal cancer cells through p53 modulation. *Cancer Chemother. Pharmacol.* **2011**, *68* (6), 1449−1457.

(29) Mhaidat, N. M.; Bouklihacene, M.; Thorne, R. F. 5-Fluorouracil-induced apoptosis in colorectal cancer cells is caspase-9-dependent and mediated by activation of protein kinase C-δ. *Oncol. Lett.* **2014**, *8* (2), 699−704.

(30) Tang, H.; Li, L.; Wang, B.; et al. Observation of antitumor mechanism of GE11-modified paclitaxel and curcumin liposomes based on cellular morphology changes. *AAPS Open* **2024**, *10* (1), 1.

(31) Zhu, G.; Shi, Q.; Cai, T.; et al. CACA guidelines for holistic integrative management of anticancer treatment-induced cutaneous adverse events. *Holistic Integr. Oncol.* **2024**, *3* (1), 33.

(32) Hermansyah, D.; Paramita, D. A.; Muhar, A. M.; et al. *Curcuma longa* extract inhibits migration by reducing MMP-9 and Rac-1 expression in highly metastatic breast cancer cells. *Res. Pharm. Sci.* **2024**, *19* (2), 157−166.

(33) Ahmad, I.; Tabrez, S. Exploring natural resources: Plumbagin as a potent anticancer agent. *S. Afr. J. Bot.* **2024**, *174*, 167−179.

(34) Sidhu, H.; Capalash, N. Plumbagin downregulates UHRF1, p-Akt, MMP-2 and suppresses survival, growth and migration of cervical cancer CaSki cells. *Toxicol. In Vitro* **2023**, *86*, No. 105512.

(35) Li, J.; Gao, H.; Wang, P.; et al. Plumbagin induces G2/M arrest and apoptosis and ferroptosis via ROS/p38 MAPK pathway in human osteosarcoma cells. *Alexandria Eng. J.* **2024**, *103*, 222−236.

(36) Hao, W.; Gao, Y.; Cao, B. Targeting Intrinsic and Extrinsic Pathways of Ferroptosis: A Novel Anticancer Strategy of Curcumin. *Pharmacogn. Mag.* **2024**, *20*, No. 09731296241251957.

(37) Ahmad, I.; Ahmad, S.; Ahmad, A.; et al. Curcumin, its derivatives, and their nanoformulations: Revolutionizing cancer treatment. *Cell Biochem. Funct.* **2024**, *42* (1), No. e3911.

(38) Kaur, C.; Sahu, S. K.; Bansal, K.; et al. Targeting Peroxisome Proliferator-Activated Receptor-β/δ, Reactive Oxygen Species and Redox Signaling with Phytocompounds for Cancer Therapy. *Antioxid. Redox Signaling* **2024**, *41* (4−6), 342−395.

(39) Sharma, B.; Dhiman, C.; Hasan, G. M.; et al. Pharmacological Features and Therapeutic Implications of Plumbagin in Cancer and Metabolic Disorders: A Narrative Review. *Nutrients* **2024**, *16* (17), 3033.

(40) Yang, Z. J.; et al. ROS-induced oxidative stress and mitochondrial dysfunction: a possible mechanism responsible for

https://doi.org/10.1021/acsomega.5c01258
ACS Omega 2025, 10, 19045−19060

noise-induced ribbon synaptic damage. *Am. J. Transl. Res.* **2024**, *16* (1), 272−284.
(41) Li, X.; Yang, C.; Wu, H.; et al. DSB-induced oxidative stress: Uncovering crosstalk between DNA damage response and cellular metabolism. *DNA Repair* **2024**, *141*, No. 103730.
(42) Tkachenko, A. Apoptosis and eryptosis: similarities and differences. *Apoptosis* **2024**, *29* (3), 482−502.
(43) Yadav, P.; Bandyopadhyay, A.; Sarkar, K. Enhancement of gold-curcumin nanoparticle mediated radiation response for improved therapy in cervical cancer: a computational approach and predictive pathway analysis. *Discover Nano* **2024**, *19* (1), 153.
(44) Rasheed, Z. Therapeutic potentials of catalase: Mechanisms, applications, and future perspectives. *Int. J. Health Sci.* **2024**, *18* (2), 1−6.
(45) Galasso, M.; Gambino, S.; Romanelli, M. G.; et al. Browsing the oldest antioxidant enzyme: catalase and its multiple regulation in cancer. *Free Radical Biol. Med.* **2021**, *172*, 264−272.
(46) Borović Šunjić, S.; Jaganjac, M.; Vlainić, J.; et al. Lipid Peroxidation-Related Redox Signaling in Osteosarcoma. *Int. J. Mol. Sci.* **2024**, *25* (8), 4559.
(47) Lai, W.; Zhang, J.; Sun, J.; et al. Oxidative stress in alcoholic liver disease, focusing on proteins, nucleic acids, and lipids: A review. *Int. J. Biol. Macromol.* **2024**, *278*, No. 134809.
(48) Xu, G.; Chen, H.; Cong, Z.; et al. Promotion of transcription factor EB-dependent autophagic process by curcumin alleviates arsenic-caused lung oxidative stress and inflammation in mice. *J. Nutr. Biochem.* **2024**, *125*, No. 109550.
(49) Li, D.; Yu, Q.; Wu, R.; et al. Interactions between oxidative stress and senescence in cancer: Mechanisms, therapeutic implications, and future perspectives. *Redox Biol.* **2024**, *73*, No. 103208.
(50) Liu, H.; Zhang, W.; Jin, L.; et al. Plumbagin Exhibits Genotoxicity and Induces G2/M Cell Cycle Arrest via ROS-Mediated Oxidative Stress and Activation of ATM-p53 Signaling Pathway in Hepatocellular Cells. *Int. J. Mol. Sci.* **2023**, *24* (7), No. 6279, DOI: 10.3390/ijms24076279.
(51) Galsky, M. D.; Guan, X.; Rishipathak, D.; et al. Immunomodulatory effects and improved outcomes with cisplatin-versus carboplatin-based chemotherapy plus atezolizumab in urothelial cancer. *Cell Rep. Med.* **2024**, *5* (2), No. 101393, DOI: 10.1016/j.xcrm.2024.101393.
(52) Chen, C. H.; Tien, N.; Yao, C.; et al. Naringin Induces ROS-Stimulated G(1) Cell-Cycle Arrest and Apoptosis in Nasopharyngeal Carcinoma Cells. *Environ. Toxicol.* **2024**, *39*, 5059−5073, DOI: 10.1002/tox.24378.
(53) Moyen Uddin Pk, M.; O'Sullivan, J.; Sayful Islam, M.; et al. Investigating the Anticancer Effects of Pleurotus ostreatus Polysaccharide on G0/G1 Cell Cycle Arrest and Apoptosis in Ehrlich Ascites Carcinoma Cells. *Chem. Biodiversity* **2024**, *21*, No. e202400897.
(54) Arango, D.; Wilson, A. J.; Shi, Q.; et al. Molecular mechanisms of action and prediction of response to oxaliplatin in colorectal cancer cells. *Br. J. Cancer* **2004**, *91* (11), 1931−1946.
(55) Güçlü, E.; et al. Piceatannol induces caspase-dependent apoptosis by modulating intracellular reactive oxygen species/mitochondrial membrane potential and enhances autophagy in neuroblastoma cells. *J. Appl. Toxicol* **2024**, *44*, 1714−1724, DOI: 10.1002/jat.4671.
(56) Shoshan-Barmatz, V.; Arif, T.; Shteinfer-Kuzmine, A. Apoptotic proteins with non-apoptotic activity: expression and function in cancer. *Apoptosis* **2023**, *28* (5), 730−753.
(57) Lev-Ari, S.; Strier, L.; Kazanov, D.; et al. Celecoxib and Curcumin Synergistically Inhibit the Growth of Colorectal Cancer Cells. *Clin. Cancer Res.* **2005**, *11* (18), 6738−6744.
(58) Petrocelli, G.; Marrazzo, P.; Bonsi, L.; et al. Plumbagin, a Natural Compound with Several Biological Effects and Anti-Inflammatory Properties. *Life* **2023**, *13* (6), 1303.
(59) Bahadar, N.; Bahadar, S.; Sajid, A.; et al. Epigallocatechin gallate and curcumin inhibit Bcl-2: a pharmacophore and docking based approach against cancer. *Breast Cancer Res.* **2024**, *26* (1), 114.
(60) Hosseini, S. S.; Reihani, R. Z.; Doustvandi, M. A.; et al. Synergistic anticancer effects of curcumin and crocin on human colorectal cancer cells. *Mol. Biol. Rep.* **2022**, *49* (9), 8741−8752.
(61) Zheng, X.; Yang, X.; Lin, J.; et al. Low curcumin concentration enhances the anticancer effect of 5-fluorouracil against colorectal cancer. *Phytomedicine* **2021**, *85*, No. 153547.
(62) Qiao, H.; Wang, T. y.; Yan, W.; et al. Synergistic suppression of human breast cancer cells by combination of plumbagin and zoledronic acid In vitro. *Acta Pharmacol. Sin.* **2015**, *36* (9), 1085−1098.
(63) Gowda, R.; Sharma, A.; Robertson, G. P. Synergistic inhibitory effects of Celecoxib and Plumbagin on melanoma tumor growth. *Cancer Lett.* **2017**, *385*, 243−250.
(64) Peng, Y.; Ao, M.; Dong, B.; et al. Anti-Inflammatory Effects of Curcumin in the Inflammatory Diseases: Status, Limitations and Countermeasures. *Drug Des., Dev. Ther.* **2021**, *15*, 4503−4525.
(65) Chang, C.; Meikle, T. G.; Drummond, C. J.; et al. Comparison of cubosomes and liposomes for the encapsulation and delivery of curcumin. *Soft Matter* **2021**, *17* (12), 3306−3313.
(66) Tian, J.-y.; Chi, C. l.; Bian, G.; et al. PSMA conjugated combinatorial liposomal formulation encapsulating genistein and plumbagin to induce apoptosis in prostate cancer cells. *Colloids Surf., B* **2021**, *203*, No. 111723.
(67) Lin, X.; Wang, Q.; Du, S.; et al. Nanoparticles for co-delivery of paclitaxel and curcumin to overcome chemoresistance against breast cancer. *J. Drug Delivery Sci. Technol.* **2023**, *79*, No. 104050.

https://doi.org/10.1021/acsomega.5c01258
ACS Omega 2025, 10, 19045−19060